

A Theoretical Approach for Passive Control of Thermoacoustic Oscillations: Application to Ducted Flames

Luca Magri¹

e-mail: lm547@cam.ac.uk

Matthew P. Juniper

e-mail: mpj1001@cam.ac.uk

Energy, Fluid Mechanics and
Turbomachinery Division,
Department of Engineering,
University of Cambridge,
Trumpington Street,
Cambridge CB2 1PZ, UK

In this paper, we develop a linear technique that predicts how the stability of a thermoacoustic system changes due to the action of a generic passive feedback device or a generic change in the base state. From this, one can calculate the passive device or base state change that most stabilizes the system. This theoretical framework, based on adjoint equations, is applied to two types of Rijke tube. The first contains an electrically heated hot wire, and the second contains a diffusion flame. Both heat sources are assumed to be compact, so that the acoustic and heat release models can be decoupled. We find that the most effective passive control device is an adiabatic mesh placed at the downstream end of the Rijke tube. We also investigate the effects of a second hot wire and a local variation of the cross-sectional area but find that both affect the frequency more than the growth rate. This application of adjoint sensitivity analysis opens up new possibilities for the passive control of thermoacoustic oscillations. For example, the influence of base state changes can be combined with other constraints, such as that the total heat release rate remains constant, in order to show how an unstable thermoacoustic system should be changed in order to make it stable. [DOI: 10.1115/1.4024957]

1 Introduction

In a thermoacoustic system, such as a flame in a tube, heat release oscillations couple with acoustic pressure oscillations. If the heat release is sufficiently in phase with the pressure, these oscillations grow, sometimes with catastrophic results [1]. Prediction and control of these oscillations is one of the most challenging questions in the design of gas turbine and rocket engines, particularly because small changes to systems can sometimes greatly influence their stability. This paper introduces a technique that identifies the most influential changes to the system and determines their effect on stability. It is applied here to two simple thermoacoustic systems. When applied to more realistic systems, it will help identify strategies for passive control of thermoacoustic oscillations.

The technique is based on adjoint sensitivity analysis, which was proposed for incompressible flows by Hill [2] and developed further by Giannetti and Luchini [3]. These authors considered the influence of a passive feedback device (the structural sensitivity), but Marquet et al. [4] extended this analysis to consider the influence of a generic change to the system (the base-state sensitivity). Sipp et al. [5] provide a comprehensive review of sensitivity analysis for incompressible fluids. Chandler et al. [6] extended this analysis to low Mach number flows in order to model variable density fluids and flames. The main goal of this paper is to extend adjoint sensitivity analysis to thermoacoustic systems, which has not been attempted before.

The systems studied in this paper are shown in Fig. 1. They are a Rijke tube containing an electrically heated hot wire [7–9], shown in Fig. 1(a), and a Rijke tube heated by a diffusion flame [10–16], shown in Fig. 1(b). Both heat sources are assumed to be compact, so that the acoustic and heat release models can be

decoupled. Both systems have three base-state parameters in common: the position of the heat source, x_h , the heat-release parameter, β , and the acoustic damping, ζ . The electrically heated Rijke tube has one further parameter: a time delay, τ , between velocity fluctuations at the wire and heat release experienced by the bulk fluid [17,18]. The diffusion flame Rijke tube has three further parameters, all of which affect the flame shape: the fuel slot width, quantified by α , the stoichiometric mixture fraction, Z_{sto} , and the Péclet number, Pe , which is the ratio of mass diffusion time scale/convection time scale.

For the structural sensitivity analysis, we investigate two different feedback mechanisms: a second heat source placed in another location along the duct and a local smooth variation of the tube cross-sectional area (Fig. 5). For the base-state sensitivity analysis, we investigate the influence of the parameters that change the shape of the flame.

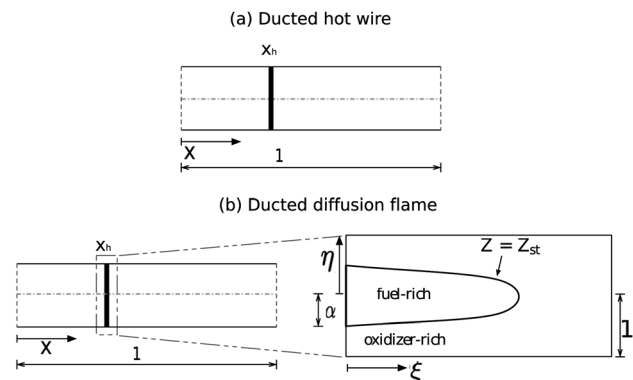


Fig. 1 Schematic of the thermoacoustic system under investigation. (a) Electrically heated Rijke tube: the hot wire is placed at $x = x_h$; (b) ducted diffusion flame: the flame is solved in the 2D domain (ξ, η) and forces the acoustics at $x = x_h$.

¹Corresponding author.

Contributed by the Controls, Diagnostics and Instrumentation Committee of ASME for publication in the JOURNAL OF ENGINEERING FOR GAS TURBINES AND POWER. Manuscript received June 27, 2013; final manuscript received July 8, 2013; published online August 21, 2013. Editor: David Wisler.

The usefulness of this technique is that a single calculation reveals how the growth rate and frequency of thermoacoustic oscillations are affected either by all possible passive control elements in the system (structural sensitivity) or by all possible changes to its base state (base-state sensitivity). Looking forward, this technique could quickly reveal, for example, the most important components of an acoustic network, the best position for an acoustic damper, or the optimal change in the flame shape. This information could be combined with optimization strategies involving other constraints, such as geometrical constraints and a given total heat release rate, to reveal the best passive strategies for stabilization of a thermoacoustic system.

2 Acoustic Model

Both thermoacoustic systems examined in this paper are horizontal Rijke tubes heated by a compact heat source. They are modeled by two different space domains: the 1D acoustic domain, in which the flame is regarded as a localized heat source, and the 2D flame domain. The acoustics are modeled in 1D, because the characteristic acoustic length is much greater than the duct width. These acoustic vibrations take place on top of a *base flow* (or *bulk fluid*), which, in this model, is constant and therefore does not enter the governing equations. The base flow only establishes some characteristic scales of the problem (see Appendix A). The dimensionless acoustic equations, called the *direct* equations, are [8,9]

$$\frac{\partial u}{\partial t} + \frac{\partial p}{\partial x} = 0 \quad (1)$$

$$\frac{\partial p}{\partial t} + \frac{\partial u}{\partial x} + \zeta p - \beta \dot{q} \delta_h = 0 \quad (2)$$

where u , p , and \dot{q} are the nondimensional velocity, pressure, and heat-release rate (scaled by β). The heat source is placed at $x = x_h$ and forces the acoustics as an impulsive term modeled with the Dirac delta $\delta_h \equiv \delta(x - x_h)$. The acoustic nondimensionalization is reported in Appendix A.

The acoustic system has three control parameters: ζ , which is the damping; β , which encapsulates all relevant information about heat release; and x_h , which is the position of the heat source. The relevant control parameters of the heat source are described in Sec. 3. At the ends of the tube, p and $\partial u / \partial x$ are both set to zero, which means that the system cannot dissipate acoustic energy by doing work on the surroundings. Dissipation and end losses are modeled with the damping parameter for each mode j , $\zeta_j = c_1 j^2 + c_2 \sqrt{j}$, where c_1 and c_2 are the damping constants. This simple damping model was used in Balasubramanian and Sujith [13], based on correlations developed by Matveev [18].

The numerical discretization is performed with the Galerkin method, choosing as basis functions the natural acoustic modes of the system, which are not the eigenfunctions of the system when the heat source is present (see Appendix B for further details). All the following results are obtained by considering six acoustic modes in the discretization. We checked modal convergence, considering more Galerkin modes. This discretization is convenient for the current study, because it is simple, but it has several drawbacks. For example, it does not account for the temperature jump across the flame and it is not readily extendable to complex acoustic networks. In future work, we will combine adjoint sensitivity analysis with an existing acoustic network model [19] in order to extend it to realistic systems.

3 Heat-Source Models

The 1D acoustics are excited by the compact heat source. Two different compact heat-source models are examined in this paper: an electrically heated hot wire and an infinite-rate chemistry diffusion flame. In this section, these two different models are briefly described.

3.1 Electrically Heated Hot Wire. A full description of a Rijke tube heated by an electrically heated hot wire, shown in Fig. 1(a), is given by Juniper [8], based on the model used by Balasubramanian and Sujith [7]. Only the dimensionless form is considered here. The heat-release rate (scaled by β) is modeled as a nonlinear time-delayed function of the velocity (Heckl [17] and Matveev [18]),

$$\dot{q} = \sqrt{\left| \frac{1}{3} + u_h(t - \tau) \right|} - \sqrt{\left| \frac{1}{3} \right|} \quad (3)$$

where u_h is the nondimensional acoustic velocity at $x = x_h$. The time delay between the pressure and heat-release oscillations is modeled by the constant time delay coefficient, τ . The hot wire is placed at $x = x_h$. Note that the resulting nondimensional heat-release rate is the product $\beta \dot{q}$. Here, the heat-release parameter β encapsulates all relevant information about the hot wire, base-flow velocity, and ambient conditions. By assuming that $|u_h(t - \tau)| \ll 1$ and $\tau \ll 2/N$, where N is the number of Galerkin modes considered for discretization, the nonlinear time-delayed heat-release term in Eq. (3) is linearized both in amplitude and time. This yields

$$\dot{q} = \frac{\sqrt{3}}{2} \left(u_h(t) - \tau \frac{\partial u_h(t)}{\partial t} \right) \quad (4)$$

3.2 Infinite-Rate Chemistry Diffusion Flame. An infinite-rate chemistry model is used for the unsteady 2D coflow diffusion flame. This assumption implies that the combustion occurs along an infinitely thin surface, where the fuel, Y , and the oxidizer, X , are at the stoichiometric ratio. The main assumptions are that the velocity field of the flame is the acoustic velocity calculated at the flame position, x_h , which is assumed to be uniform within the 2D combustion domain; the flame at any instant is located at the stoichiometric surface; and the Lewis number is 1.

The stoichiometric mass ratio is $s = \nu_x W_x / \nu_y W_y$, where W_x and W_y are the molar mass ([kg/mole]) and ν_x and ν_y ([mole/kg]) are the stoichiometric coefficients of the oxidizer and fuel, respectively. In order to make this problem easier for numerical treatment, it is useful to define the conservative scalar variable Z , also known as Schvab-Zel'dovich variable,

$$Z \equiv \frac{Y - X + X_i}{X_i + Y_i} \quad (5)$$

where X is the oxidizer mass fraction divided by $\nu_x W_x$ and Y is the fuel mass fraction divided by $\nu_y W_y$. The stoichiometric surface, where the whole reaction occurs, is the locus of points in which Z assumes the stoichiometric value $Z_{sto} = 1/(1 + \phi)$, where $\phi \equiv Y_i/X_i$ is the *equivalence ratio* [20]. The parabolic partial differential equation governing the mixture fraction Z , in nondimensional form, is

$$\frac{\partial Z}{\partial t} + (1 + u_h) \frac{\partial Z}{\partial \xi} = \frac{1}{Pe} \left(\frac{\partial^2 Z}{\partial \xi^2} + \frac{\partial^2 Z}{\partial \eta^2} \right) \quad (6)$$

along with the relevant boundary conditions, $Z(\xi = 0, \eta) = 1$, when $|\eta| \leq \alpha$; $Z(\xi = 0, \eta) = 0$, when $\alpha < |\eta| \leq 1$; $(\partial Z / \partial \eta)(\xi, \eta = \pm 1) = 0$; and $(\partial Z / \partial \xi)(\xi = L_c, \eta) = 0$.

u_h is the acoustic velocity evaluated at the acoustic flame location, x_h , such that $|u_h| \ll 1$; Pe is the Péclet number, and α is the nondimensional fuel slot half width. The nondimensional combustion parameters are reported in Appendix A.

The variable Z is split into two components: $Z = \bar{Z} + \varepsilon z$, where \bar{Z} is the analytical steady solution (Appendix C, Eq. (C1)), and εz is the unsteady field. In fully nonlinear analysis, where no approximation is made, $\varepsilon = 1$. In linear analysis, the unsteady component is considered to be very small, $|\varepsilon| \ll 1$, so that the

higher order term $\epsilon u_h \partial z / \partial \xi \sim 0$ is discarded. The problem linearized about a steady state is, therefore,

$$\frac{\partial \bar{Z}}{\partial \xi} - \frac{1}{Pe} \left(\frac{\partial^2 \bar{Z}}{\partial \xi^2} + \frac{\partial^2 \bar{Z}}{\partial \eta^2} \right) = 0 \quad (7)$$

$$\frac{\partial z}{\partial t} + \frac{\partial z}{\partial \xi} - \frac{1}{Pe} \left(\frac{\partial^2 z}{\partial \xi^2} + \frac{\partial^2 z}{\partial \eta^2} \right) + u_h \frac{\partial \bar{Z}}{\partial \xi} = 0 \quad (8)$$

Importantly, \bar{Z} has the same boundary condition as Z . The unsteady component z at the inlet, $\xi = 0$, must be zero. A detailed derivation of this equation is given by Refs. [10–16].

3.2.1 Heat Release Rate. In the energy equation, Eq. (2), the heat release rate acts as a forcing term. The total heat release rate is given by the integral over the combustion space domain (ξ, η) of the total derivative of the sensible enthalpy, namely

$$\dot{Q} = \int_R \frac{d(T_b - T_i)}{dt} d\xi d\eta \quad (9)$$

where $T_b = T_i + Z$, if $Z < Z_{sto}$, and $T_b = T_i + Z_{sto}(1 - Z)/(1 - Z_{sto})$, if $Z \geq Z_{sto}$. The nondimensional combustion space domain, in which the flame is solved, is $R \equiv [0, L_c] \times [-1, 1]$. The steady heat release rate depends on whether the flame is closed (overventilated), $Z_{sto} > \alpha$, or open (underventilated), $Z_{sto} < \alpha$. It is $\bar{Q} = 2\alpha$ and $\bar{Q} = 2(Z_{sto}/(1 - Z_{sto}))(1 - \alpha)$, respectively. For both cases, the flame tends to assume constant height (infinite length) in the limit $Z_{sto} \rightarrow \alpha$. Hence, if the flame is open, the length tends to increase if Z_{sto} increases, and vice versa if the flame is closed (Fig. 8(a)). For the acoustic energy equation, Eq. (2), we need to evaluate the fluctuating averaged heat release rate which, with Galerkin discretization, is given by

$$\dot{q} \equiv \dot{Q} - \bar{Q} = \int_0^{L_c} \int_{-1}^1 \theta(Z > Z_{sto}) \left(\frac{-1}{1 - Z_{sto}} \right) \frac{\partial z}{\partial t} d\xi d\eta + u_h \bar{Q} \quad (10)$$

where $\theta(Z > Z_{sto})$ is the step function, which is 1 in the fuel side $Z > Z_{sto}$ and 0 otherwise. We emphasize that the above expression is valid for both closed and open flames. Numerical treatment of this flame is outlined in Appendix B and, in a slightly different formulation, in Balasubramanian and Sujith [13]. Magri and Juniper [14] and Magri et al. [16] will contain further details. The non-dimensionalization of the flame-domain parameters is reported in Appendix A.

4 Adjoint Operator

In this section, the *adjoint operator* is defined. Let Θ be a partial differential operator of order M acting on the function $f(x_1, x_2, \dots, x_K, t)$, where K is the space dimension, such that $\Theta f(x_1, x_2, \dots, x_K, t) = 0$. We refer to the operator Θ as the *direct operator* and the function f as the *direct variable*. The adjoint operator Θ^+ and adjoint variable f^+ are defined via the *generalized Green's identity* (see Magri and Juniper [9]),

$$\int_0^T \int_V f^{++} \Theta f - f(\Theta^+ f^+)^* dV dt = \int_0^T \int_S \sum_{i=1}^K \left[\frac{\partial}{\partial x_i} F_i(f, f^{++}) \right] n_i dS dt + \int_V F_i(f, f^{++})|_0^T dV \quad (11)$$

where $i = 1, 2, \dots, K$ and $F_i(f, f^{++})$ are functions that depend bilinearly on f, f^{++} , and their first $M-1$ derivatives. The complex-conjugate operation is labeled by $*$. The domain V is enclosed by the surface S , for which n_i are the projections on the coordinate

axis of the unit vector in the direction of the outward normal to the surface dS . The time interval is T . The adjoint boundary conditions and initial conditions of the function f^+ are defined as those that make the RHS in Eq. (11) vanish identically on S , $t = 0$, and $t = T$.

The adjoint equations can either be derived from the continuous direct equations and then discretized (*CA*, discretization of the continuous adjoint) or be derived directly from the discretized direct equations (*DA*, discrete adjoint). For the *CA* method, the adjoint equations are derived by integrating the continuous direct equations by parts and then applying Green's identity from Eq. (11). They are then discretized with the Galerkin method. For the *DA* method, the adjoint system is simply the negative Hermitian of the direct matrix: $\Phi_{ij} = -\Gamma_{ji}^*$ [9].

In Magri and Juniper [9], a comparison between the numerical truncation errors of the two above methods is illustrated. For the thermoacoustic systems considered in this paper, the *DA* method is more accurate and easier to implement. We use both the *CA* and *DA* methods for the first thermoacoustic system, an electrically heated Rijke tube, while we use only the *DA* method for the second thermoacoustic system, a ducted diffusion flame. However, the continuous adjoint equations *CA* of the latter system will be available in Magri and Juniper [14].

The continuous adjoint equations of the electrically heated Rijke tube, Eqs. (1), (2), and (4), are

$$\frac{\partial u^+}{\partial t} + \frac{\partial p^+}{\partial x} + \frac{\sqrt{3}}{2} \beta \left(p_h^+ + \tau \frac{\partial p_h^+}{\partial t} \right) \delta_h = 0 \quad (12)$$

$$\frac{\partial u^+}{\partial x} + \frac{\partial p^+}{\partial t} - \zeta p^+ = 0 \quad (13)$$

These adjoint equations govern the evolution of the adjoint variables, which can be regarded as Lagrange multipliers from a constrained optimization perspective. Hence, u^+ is the Lagrange multiplier of the acoustic momentum equation, Eq. (1). Physically, it reveals the locations where the system is most sensitive to a given force acting on the acoustic momentum. Likewise, p^+ is the Lagrange multiplier of the energy equation, Eq. (2). Physically, it reveals the locations where the system is most sensitive to a given heat injection.

5 Optimal Passive Control via Adjoint Structural Sensitivity

We define a passive device to be an object that causes feedback between the state variables and the governing equations at the position where it is placed. In the language of active control, the sensor and actuator are colocated and there is a fixed relationship between the observation (which is derived from the state variables at that point) and the actuation (the forcing terms in the governing equations). For example, the flame holder of an unlit afterburner can be thought of as a passive device in which the drag exerts a force on the fluid in the opposite direction to the velocity at that point.

5.1 Structural Sensitivity to a Generic Feedback Device.

By working out the four components of the structural sensitivity tensor, we can calculate the effect of any passive feedback device and thereby identify the device that is most effective at changing the frequency or growth rate of the system. In this section, the direct and adjoint eigenfunctions are computed by considering a hot wire as a heat source. The parameters are such that the first acoustic mode is the most unstable, but the analysis can be repeated for the cases when second or higher modes are most unstable [9]. An analytical formula for the structural sensitivity tensor is obtained as follows:

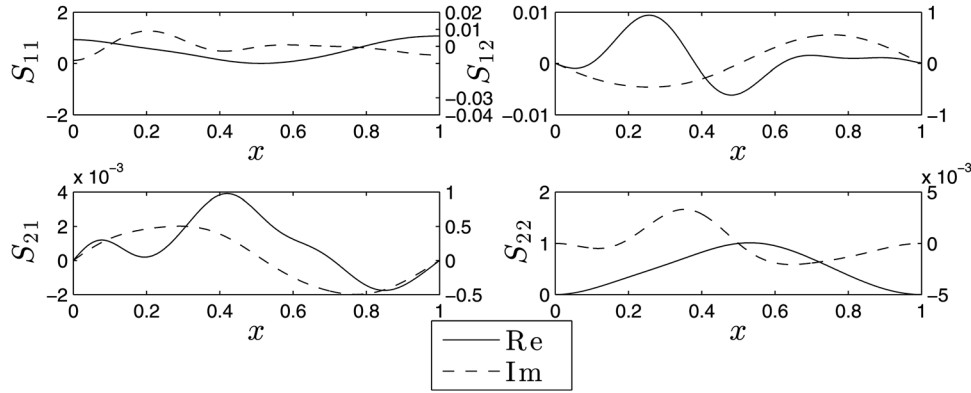


Fig. 2 Structural sensitivity tensor. Each component quantifies the effect of a feedback mechanism on the linear growth rate (solid line/left scale) and angular frequency (dashed line/right scale) of the oscillations. $c_1 = 0.01$, $c_2 = 0.001$, $\tau = 0.01$, $\beta = 0.39$, $x_h = 0.25$.

- Consider an eigenvalue problem by inserting the following transformations into the direct and adjoint equations, Eqs. (1), (2), and (12), (13), respectively:

$$u(x, t) = \hat{u}(x, \sigma)e^{\sigma t}, \quad u^+(x, t) = \hat{u}^+(x, \sigma)e^{-\sigma^* t} \quad (14)$$

$$p(x, t) = \hat{p}(x, \sigma)e^{\sigma t}, \quad p^+(x, t) = \hat{p}^+(x, \sigma)e^{-\sigma^* t} \quad (15)$$

Consequently, the direct eigenvalue problem is

$$\sigma \hat{u} + \frac{\partial \hat{p}}{\partial x} = 0 \quad (16)$$

$$\sigma \hat{p} + \frac{\partial \hat{u}}{\partial x} + \zeta \hat{p} - \frac{\sqrt{3}}{2} \beta (\hat{u}_h - \tau \sigma \hat{u}_h) \delta_h = 0 \quad (17)$$

while the adjoint eigenvalue problem becomes

$$-\sigma^* \hat{u}^+ + \frac{\partial \hat{p}^+}{\partial x} + \frac{\sqrt{3}}{2} \beta (\hat{p}_h^+ - \tau \sigma^* \hat{p}_h^+) \delta_h = 0 \quad (18)$$

$$-\sigma^* \hat{p}^+ + \frac{\partial \hat{u}^+}{\partial x} - \zeta \hat{p}^+ = 0 \quad (19)$$

- Perturb the direct equations, Eqs. (16) and (17) by a generic, constant, small, localized feedback mechanism δC proportional to the state variables, where δC is represented by a 2×2 matrix
- Assume that the perturbation is small enough for the new thermoacoustic configuration, such that $\sigma_{\text{new}} = \sigma + \delta\sigma$, $\hat{p}_{\text{new}} = \hat{p} + \delta\hat{p}$, and $\hat{u}_{\text{new}} = \hat{u} + \delta\hat{u}$, where $\delta\sigma \sim \varepsilon\sigma$, $\delta\hat{p} \sim \varepsilon\hat{p}$, and $\delta\hat{u} \sim \varepsilon\hat{u}$ with $|\varepsilon| \ll 1$ and where terms of order ε^2 are sufficiently small to be neglected. Therefore, only terms $\sim O(\varepsilon^1)$ or smaller are retained. Accordingly, the perturbed direct eigenvalue problem is governed by the following equations:

$$\sigma \delta \hat{u} + \frac{\partial \delta \hat{p}}{\partial x} = -\delta \sigma \hat{u} + \delta C_{11} \delta_c \hat{u} + \delta C_{12} \delta_c \hat{p} \quad (20)$$

$$\begin{aligned} \sigma \delta \hat{p} + \frac{\partial \delta \hat{u}}{\partial x} - \frac{\sqrt{3}}{2} \beta (1 - \sigma \tau) \delta \hat{u}_h \delta_h + \zeta \delta \hat{p} \\ = \delta C_{21} \delta_c \hat{u} + \delta C_{22} \delta_c \hat{p} - \delta \sigma \hat{p} - \frac{\sqrt{3}}{2} \beta \tau \hat{u}_h \delta \sigma \delta_h \end{aligned} \quad (21)$$

- Multiply Eqs. (20) and (21) by \hat{u}^{+*} and \hat{p}^{+*} , respectively; multiply the complex conjugate of the adjoint eigenvalue problem in Eqs. (18) and (19) by $\delta \hat{u}$ and $\delta \hat{p}$, respectively; and sum together. By integrating over the duct length

(nondimensionalized, such that it is unitary), we obtain an explicit formula for the *structural sensitivity tensor*, $S_{ij} = \delta\sigma / \delta C_{ij}$, which is

$$S \equiv \frac{\delta\sigma}{\delta C} = \frac{[\hat{u}^{+*}, \hat{p}^{+*}]^T \otimes [\hat{u}, \hat{p}]^T}{\int_0^1 (\hat{u} \hat{u}^{+*} + \hat{p} \hat{p}^{+*}) dx + \frac{\sqrt{3}}{2} \beta \tau \hat{u}_h \hat{p}_h^{+*}} \quad (22)$$

The direct and conjugate adjoint eigenfunctions are arranged as column vectors $[\hat{u}, \hat{p}]^T$ and $[\hat{u}^{+*}, \hat{p}^{+*}]^T$, respectively. In general, a structural perturbation to the thermoacoustic operator can be represented by a 2×2 tensor, which acts on $[\hat{u}, \hat{p}]^T$. Each component of this structural perturbation tensor quantifies the effect of a feedback mechanism between the j th eigenfunction and the i th governing equation. The four components of S quantify how a feedback mechanism that is proportional to the state variables affects the growth rate and frequency of the system. They are shown in Fig. 2 as a function of x , which is the location where the passive device (structural perturbation) sits. They are explained physically below.

Firstly ($S_{11} = \hat{u} \hat{u}^{+*}$), we consider a force in the momentum equation that is proportional to the velocity at a given point. For example, this could be the (linearized) drag force about an obstacle in the flow. This type of feedback greatly affects the growth rate but hardly affects the frequency. It has most influence when it is at the entrance or exit of the duct. This is because (i) the velocity eigenfunction is maximal there and (ii) the adjoint velocity, which is a measure of the sensitivity of the momentum equation, is also maximal there (shown in Magri and Juniper [9]). The real part of S_{11} is positive for all values of x , which means that, whatever value of x is chosen, the growth rate will decrease if the forcing is in the opposite direction to the velocity. This tells us that the drag force about an obstacle in the flow will always stabilize the thermoacoustic oscillations but is most effective if placed at the upstream or downstream end of this duct. Furthermore, by inspection of the amplitudes of the black lines in Fig. 2, we see that this is the most effective passive device.

Secondly ($S_{22} = \hat{p} \hat{p}^{+*}$), we consider a feedback mechanism that is proportional to the pressure and that forces the energy equation. The pressure-coupled heat release described in Chu [21], which arises in solid rocket engines, is an example of this type of feedback. For this feedback, the system is most sensitive around the center of the duct. As for S_{11} , this feedback greatly affects the growth rate but hardly affects the frequency and is positive for all values of x . If the heat release increases with the pressure, as it does for most chemical reactions, this feedback mechanism is destabilizing. But if a fuel could be found with the opposite

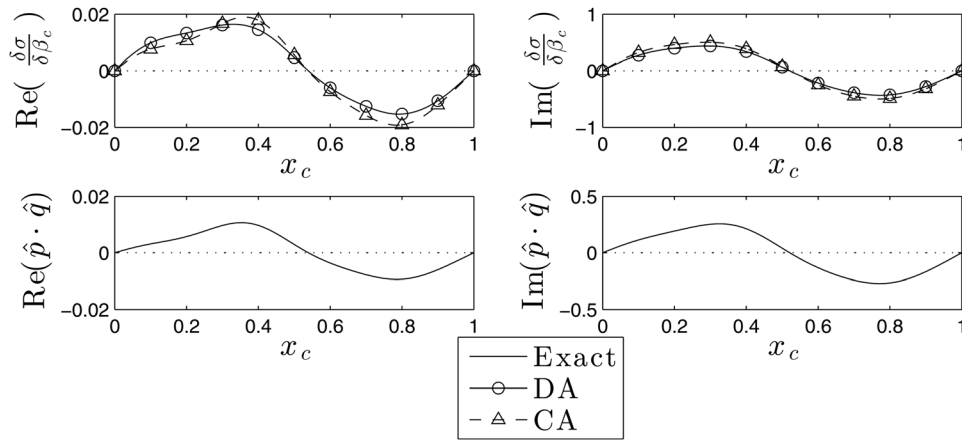


Fig. 3 Top frames: structural sensitivity of the growth rate, $\text{Re}(\delta\sigma/\delta\beta_c)$, and of the angular frequency, $\text{Im}(\delta\sigma/\delta\beta_c)$, when a control hot wire is placed at position x_c . Bottom frames: Rayleigh index for a control wire placed at x_c . System parameters as in Fig. 2.

behavior, then it would most stabilize the oscillations if placed at the center of the duct.

Thirdly ($S_{12} = \hat{p}\hat{u}^{+*}$), we consider feedback from the pressure into the momentum equation and ($S_{21} = \hat{u}\hat{p}^{+*}$) feedback from the velocity into the energy equation. These types of feedback hardly affect the growth rate but greatly affect the frequency. A control hot wire with $\tau \approx 0$ causes this type of feedback (S_{21}), so this analysis shows that it will be relatively ineffective at stabilizing thermoacoustic oscillations.

5.2 Structural Sensitivity to a Control Hot Wire. In

Sec. 5.1, we showed that the components of the structural sensitivity tell us the effect of any passive control device, as long as we know how the device affects the flow around it. In this section, we illustrate this for a second hot wire, denoted with the subscript c , even though it is a relatively ineffective device. We compare the structural sensitivity results with those calculated using the Rayleigh index and then demonstrate numerically that this can restabilize an unstable thermoacoustic system.

The feedback from the control wire is proportional to the velocity perturbation and perturbs the energy equation. The structural perturbation tensor therefore has only one component: $\delta C_{21} = \delta\beta_c(1 - \sigma\tau_c)$. The sensitivity to the presence of a control hot wire placed at $x = x_c$ is given by the following formula:

$$\frac{\delta\sigma}{\delta\beta_c} = \frac{\hat{p}_c^{+*}\hat{u}_c(1 - \sigma\tau_c)}{\int_0^1 (\hat{u}\hat{u}^{+*} + \hat{p}\hat{p}^{+*})dx + \frac{\sqrt{3}}{2}\beta\tau\hat{u}_h\hat{p}_h^{+*}} \quad (23)$$

It has long been known that, if pressure and heat-release fluctuations are in phase, then acoustic vibrations are encouraged. More precisely, the Rayleigh criterion [22] states that the energy of the acoustic field grows over one cycle of oscillation if $\oint_T \int_D p\dot{q}dDdt$ exceeds the damping, where \mathcal{D} is the flow domain and T is the period. It is particularly informative to plot the spatial distribution of

$$\oint_T p\dot{q}dt \quad (24)$$

which is known as the Rayleigh index. This reveals the regions of the flow that contribute most to the Rayleigh criterion and therefore gives insight into the physical mechanisms that alter the amplitude of the oscillation. To examine the effect of the control wire, we substitute the approximate expressions $p = \hat{p}\exp(\sigma_i t)$ and $\dot{q} = \hat{q}\exp(\sigma_i t)$ into Eq. (24) and integrate over a period $2\pi/\sigma_i$, where $\sigma_i = \text{Im}(\sigma)$. (The approximation arises because the

growth rate over the cycle has been ignored.) As expected, the sign of the Rayleigh index (bottom frames in Fig. 3) matches that of the structural sensitivity (top frames in Fig. 3), and the shape is similar.

The Rayleigh index physically explains the effect of adding the control hot wire to the Rijke tube: for $x_c = 0-0.54$, the pressure and heat-release eigenfunctions are sufficiently in phase that the contribution to growth over a cycle is positive; and for $x_c = 0.54-1$, they are out of phase, so their contribution to growth over a cycle is negative. It is interesting to note that this system becomes more unstable when the control wire is placed at $0.5 < x_c < 0.54$. This is in the second half of the tube and, in the absence of the first hot wire, a control wire placed here would be stabilizing. The reason for this is that the main hot wire, at x_h , causes the eigenfunctions to distort from the acoustic modes of the duct. In particular, the features of the \hat{u} and \hat{p} eigenfunctions shift down the duct to higher values of x_c . This shifts downstream the region in which the control wire is destabilizing.

We demonstrate the suppression of thermoacoustic oscillations using a control wire placed at the optimal location, as predicted by the structural sensitivity analysis. We use the parameters in Fig. 3, which shows that, in order to reduce the growth rate most effectively, the control wire should be placed at $x_c = 0.8$. We integrate the nonlinear time-delayed governing equations, Eqs. (1)–(3) forward in time with a fourth order Runge–Kutta algorithm. When the control wire is absent, the growth rate is $\sigma_r = 1.91 \times 10^{-5}$ (near the Hopf bifurcation point) and the angular frequency is $\sigma_i = 3.309$. We set the heat-release parameter for the control wire to be $\beta_c = \beta/10 = 0.039$, which is small enough to fulfill the linear assumptions. When the control wire is present, the growth rate is $\sigma_r = -2.15 \times 10^{-4}$ and the angular frequency is $\sigma_i = 3.292$. The difference between these values matches that predicted by the structural sensitivity analysis, for which $\delta\sigma = \beta_c \times \delta\sigma/\delta\beta_c \approx 0.039 \times (-0.01528 - 0.425i) = -5.79 \times 10^{-4} - 0.0166i$ at $x_c = 0.8$.

Figure 4(a) shows the pressure as a function of time in the nonlinear simulations. The control wire is introduced at $t = 1000$. The behavior is as predicted: there is stable nonlinear oscillation until $t = 1000$ and exponential decay afterwards. Figures 4(b) and 4(c) show the fast Fourier transform. These figures confirm the frequency shift and stabilization predicted by the structural sensitivity analysis but at much greater numerical expense.

5.3 Structural Sensitivity to Smooth Cross-Sectional Area Variation. For smooth variations of the cross-sectional area, the nondimensional energy equations, Eqs. (2)–(4) can be rewritten [23–25] as

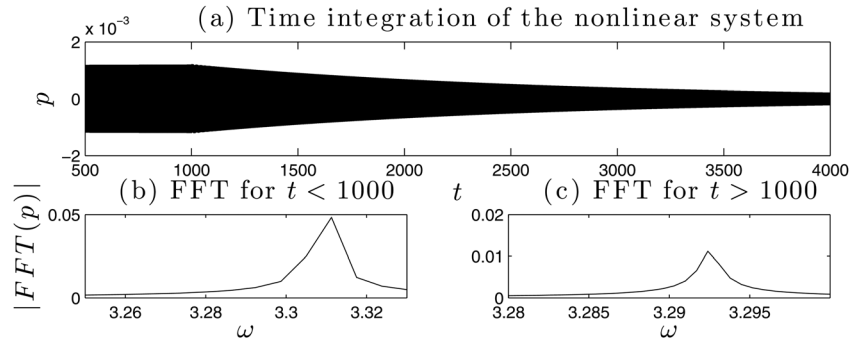


Fig. 4 Stabilization with a control wire introduced at $t = 1000$ and placed at optimal position $x_c = 0.8$ predicted by adjoint analysis. System parameters as in Fig. 2, $\beta_c = \beta/10$.

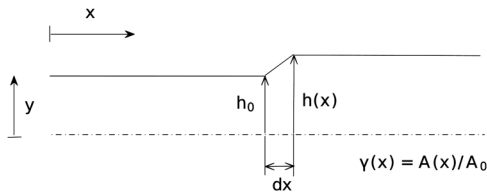


Fig. 5 An infinitesimal variation of the cross-sectional area $A(x)$ of the Rijke tube is regarded as a localized feedback mechanism for passive control

$$\frac{\partial p}{\partial t} + \frac{\partial u}{\partial x} + \zeta p - \frac{\sqrt{3}}{2} \beta \left(u_h - \tau \frac{\partial u_h}{\partial t} \right) \delta_h = -u \frac{1}{\gamma} \frac{\partial \gamma}{\partial x} \quad (25)$$

with $\gamma \equiv A(x)/A_0$, where $A(x)$ is the area at location x of height $h(x)$ and A_0 is the area at the mouth of the duct of height h_0 , as sketched in Fig. 5. If γ varies, the RHS of Eq. (25) shows that a change in the area can be interpreted as a forcing term, proportional to $-u$, acting on the energy equation. We assume that the area of the duct is constant, except at location $x = x_c$, where there is a small smooth change in the area. The structural perturbation is proportional to the acoustic velocity, $-u_c$, and affects the energy equation, which becomes

$$\frac{\partial p}{\partial t} + \frac{\partial u}{\partial x} + \zeta p - \frac{\sqrt{3}}{2} \beta \left(u_h - \tau \frac{\partial u_h}{\partial t} \right) \delta_h = -u_c \frac{1}{\gamma} \frac{\partial \gamma}{\partial x} \theta_c \quad (26)$$

where θ_c is one at $x = x_c$ and zero elsewhere. A “local smooth cross-sectional area variation” is defined such that $\partial \gamma / \partial x \theta_c$ is finite. The structural sensitivity is provided by the negative of S_{21} in Eq. (22). Therefore, the eigenvalue drift caused by this feedback mechanism is $\delta \sigma = -(\partial \gamma / \partial x) S_{21} (1/\gamma)$. This means that, where a control hot wire has a stabilizing effect, a positive change in area in the same location has a destabilizing effect and vice versa.

6 Base-State Sensitivity

The structural sensitivity gives the effect of adding a passive feedback device to the system. The base-state sensitivity gives the effect of altering the thermoacoustic system without adding any passive devices. This is likely to be more interesting in practice. The base-state sensitivity is calculated directly from the discretized governing equations (the DA method). There are four stages in this method: (1) calculate the perturbation matrix $\delta \Gamma$, by imposing an arbitrarily small perturbation on the base-state parameter; (2) calculate the eigenvectors of the direct matrix, Γ , and adjoint matrix, Φ ; (3) apply the formula in Eq. (27) to find the eigenvalue

drift; and (4) divide the eigenvalue drift by the small perturbation used to produce $\delta \Gamma$ at step 1. It can be shown (see, for instance, Ref. [3]) that the eigenvalue drift due to a perturbation of the discretized direct system is given by

$$\delta \sigma = \frac{\hat{\xi}^* \cdot (\delta \Gamma \hat{\zeta})}{\hat{\xi}^* \cdot \hat{\zeta}} \quad (27)$$

The column vector $\hat{\zeta}$ is the eigenvector of the direct matrix Γ , while $\hat{\xi}^*$ is the eigenvector of the adjoint matrix $\Phi_{ij} = -\Gamma_{ji}^*$. Here, we demonstrate the base-state sensitivity for the electrically heated Rijke tube and the ducted diffusion flame.

6.1 Electrically Heated Hot Wire. The top frames of Fig. 6 show how a variation in the heat-release parameter, β , affects the growth rate, $\text{Re}(\sigma)$, and the angular frequency, $\text{Im}(\sigma) \equiv \omega$, for different hot wire positions, x_h . The bottom frames of Fig. 6 show how a variation in the time-delay coefficient, τ , affects the same quantities. These are calculated via the DA method, and the result is checked against the exact solution, which is obtained by finite difference.

We see that small variations in β have a much greater effect on the frequency than on the growth rate, while small variations in τ have a much greater effect on the growth rate than on the frequency. In other words, the growth rate is extremely sensitive to the time delay in the model. This is a well-known result, and the reasons for this are discussed in Ref. [9]. Its value here is in the successful demonstration of the method.

6.2 Infinite-Rate Chemistry Diffusion Flame. In this section, the base-state sensitivity analysis is used to calculate how the flame shape affects the growth rate and frequency of the thermoacoustic oscillations. This is a particularly interesting application because combustion technologists have some control over the flame shape. In this model, the flame shape is determined by the Péclet number, Pe , the stoichiometric mixture fraction, Z_{sto} , and the duct width, α . Here, the heat-release parameter is fixed at $\beta = 0.67/2$ and the flame position at $x_h = 0.25$, at which point this thermoacoustic system is marginally stable when $Pe = 35$, $Z_{\text{sto}} = 0.8$, and $\alpha = 0.35$ [26]. Maps of the base-state sensitivity are shown in Fig. 7 with $\alpha = 0.35$, which correspond to overventilated (i.e., closed) flames, because $Z_{\text{sto}} > \alpha$. In the left frames, the color scale shows the rate of change of growth rate with Z_{sto} (top left) and with Pe (bottom left) as a function of the base-state values of Pe and Z_{sto} . In the right frames, the color scale shows the rate of change of the angular frequency with Z_{sto} (top right) and with Pe (bottom right). These have been checked against the exact solutions obtained (expensively) via finite difference and agree to a tolerance of 10^{-9} . Further details on the parameters used and the numerical treatment will be available in Magri and Juniper [14].

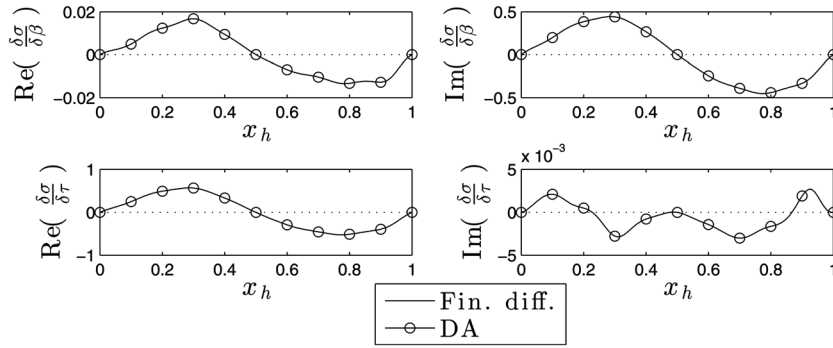


Fig. 6 Hot wire as heat source: sensitivity to base-state modifications. System parameters as in Fig. 2.

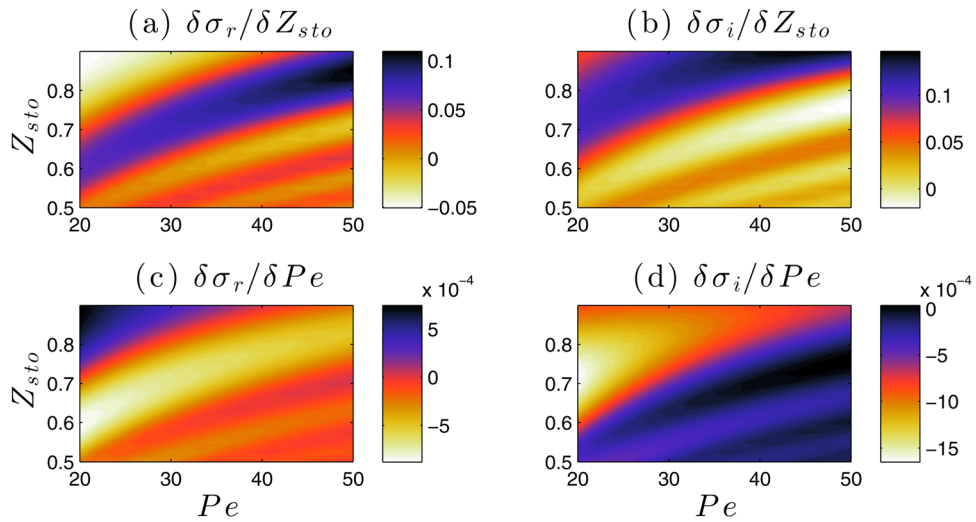


Fig. 7 Diffusion flame as heat source: sensitivity to base-state modifications of Z_{sto} and Pe

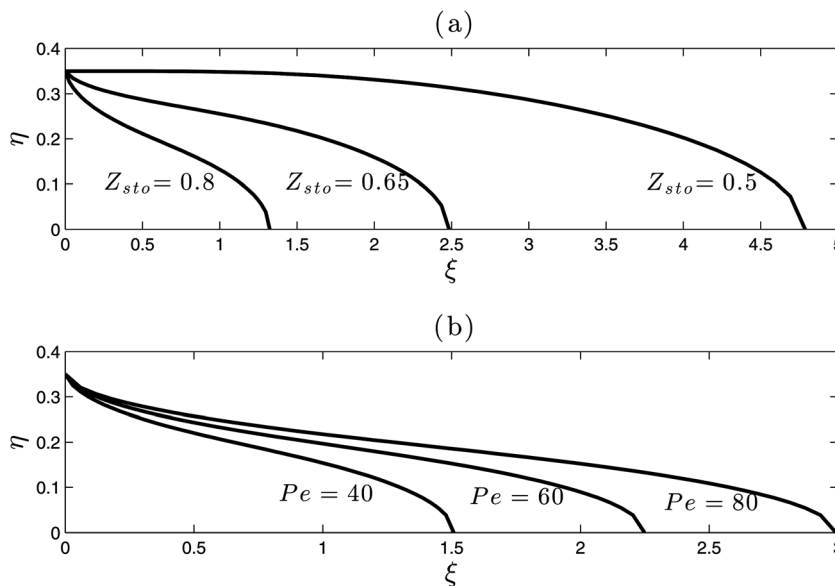


Fig. 8 Flame shape, represented by the stoichiometric curve, as a function of Z_{sto} (a) and Pe (b). In the top frame, $Pe = 60$; in the bottom frame, $Z_{sto} = 0.8$.

Figure 7 shows that the stability of the system is much more sensitive to the stoichiometric mixture fraction, Z_{sto} , than to the Péclet number. The sensitivities show that, around these operating points: (i) at a given Pe , small increases of δZ_{sto} , which tend to shorten the flame (Fig. 8(a)), make the system more stable when the unperturbed flame is sufficiently short (light colors, Fig. 7(a)) and increase the oscillation frequency, regardless of the flame length (Fig. 7(b)); (ii) at a given Z_{sto} , small increases of δPe , which tend to lengthen the flame (Fig. 8(b)), make the system more stable when the flame is long (light colors, Fig. 7(c)) but decrease the angular frequency in any case (Fig. 7(d)); and (iii) the thermoacoustic system is more sensitive to changes of δZ_{sto} but less sensitive to changes of δPe . Similar results can be derived for variations of the other three parameters: x_h , α , and β . This base-state sensitivity analysis therefore allows a combustion technologist to quickly examine the stability of a given model and how the stability varies with the parameters of the model over a wide range of parameter space. On a cautionary note, the results are, of course, only as good as the model from which they are derived.

7 Conclusions

The aim of this paper is to extend adjoint sensitivity analysis to thermoacoustic systems. We consider a Rijke tube containing an electrically heated wire and a Rijke tube containing a diffusion flame. By combining information from the direct and adjoint equations, we predict how the least stable/most unstable eigenvalue of these thermoacoustic systems changes when a generic passive feedback device is introduced. From this, we find that devices that exert a drag force on the fluid have the biggest effect on the growth rate.

Two physical feedback mechanisms in particular are investigated: a second heat source placed in another location along the duct (a second hot wire) and a local smooth variation of the tube cross-sectional area. We find that these feedback mechanisms have more effect on the frequency of oscillations than on their growth rate. For the first of these systems, we verify the predictions from the adjoint analysis by comparing them with the results of time integration of the fully nonlinear system.

In the base-state sensitivity analysis, we investigate how tiny variations in the base-state parameters affect the most unstable eigenvalue of the system. This reveals how best to change these parameters in order to stabilize the system and also which base-state parameters have most influence on the stability. For the electrically heated Rijke tube, we find that (i) the system is more sensitive to small variations of the time-delay coefficient, τ , than it is to the heat-release term, β , and (ii) a change of β is more effective for control of the frequency, whereas a change in τ is more effective for control of growth rate. For the diffusion flame Rijke tube close to a Hopf bifurcation, we find that (i) the system is much more sensitive to small fluctuations of the stoichiometric mixture fraction, δZ_{sto} , than to the Péclet number and (ii) the growth rate is very sensitive to small changes of δZ_{sto} and therefore the flame length, with stabilizing effect when the unperturbed flame is short.

The sensitivity analysis proposed in this paper has been carried out by linearizing the nonlinear governing equations around fixed points. Therefore, we have studied how to extend the linear stable region of fixed points by changing some parameters of the system or introducing passive devices. In future work, we will apply adjoint Floquet analysis to study the stability and control of nonlinear self-sustained oscillations by linearizing the equations around these periodic solutions. We will also examine more realistic acoustic networks with a state-space implementation of an acoustic-network model [19]. The successful application of sensitivity analysis to more realistic thermoacoustic models will open up new possibilities for the design of passive control strategies for thermoacoustic oscillations.

Acknowledgment

The authors would like to thank Professor R. I. Sujith (IIT Madras, Chennai, India) and Dr. K. Balasubramanian (State University of New York) for helpful discussions on the Galerkin method. L.M. is financially supported by the European Research Council through Project ALORS 2590620. L.M. is grateful to Homerton College and Cambridge Philosophical Society for allocating research grants in support of travel costs for the ASME Turbo Expo Conference 2013, San Antonio, TX.

Nomenclature

c_1, c_2	= damping coefficients
CA	= continuous adjoint
DA	= discrete adjoint
i	= imaginary unit, $i^2 = -1$
p	= acoustic pressure
Pe	= Péclet number
\dot{q}	= heat-release rate divided by β
S	= structural sensitivity tensor
u	= acoustic velocity
X	= oxidizer mass fraction
Y	= fuel mass fraction
Z	= mixture fraction
Z_{sto}	= stoichiometric mixture fraction
\otimes	= dyadic product
$\hat{}$	= eigenfunction or eigenvector

Greek Symbols

α	= nondimensional fuel slot half width
β	= heat-release parameter
δ_k	= Dirac δ , $\delta_k \equiv \delta(x - x_k)$
Γ	= direct matrix
ζ	= damping factor
σ	= complex eigenvalue, $\sigma_r + i\sigma_i$
τ	= time-delay coefficient
Φ	= adjoint matrix
ϕ	= equivalence ratio
χ	= direct state vector

Subscripts

c	= passive control device
h	= heat source
i	= inlet of the diffusion flame
x	= oxidizer
y	= fuel

Superscripts

$+$	= adjoint
$*$	= complex conjugate

Appendix A: Scale Factors for Nondimensionalization

Dimensional quantities are denoted with \sim . The acoustic variables are scaled as $\tilde{L}_a x = \tilde{x}$ [m], $\tilde{L}_a t_{ac} / \tilde{c}_0 = \tilde{t}$ [s], $\tilde{U}_0 u = \tilde{u}$ [m/s], and $\gamma M \tilde{p}_0 p = \tilde{p}$ [Pa], where \tilde{L}_a [m] is the length of the Rijke tube, \tilde{c}_0 [m/s] is the speed of sound in the base flow, \tilde{U}_0 [m/s] is the base-flow velocity, \tilde{p}_0 [Pa] is the base-flow pressure, $\gamma = \tilde{c}_p / \tilde{c}_v$, and M is the base-flow Mach number. \tilde{c}_p and \tilde{c}_v are the mass heat capacities at constant pressure and constant volume of the mixture [$\text{Jkg}^{-1}\text{K}^{-1}$], respectively.

In the ducted diffusion flame, the combustion variables are scaled as $\tilde{H}\tilde{\xi} = \tilde{\xi}$ [m], $\tilde{H}\tilde{\eta} = \tilde{\eta}$ [m], $\tilde{H}t_c / \tilde{U}_0 = \tilde{t}$ [s], and $\tilde{T}_{ref} T = \tilde{T}$ [K], where \tilde{H} is the fuel slot half width, $\tilde{T}_{ref} = \tilde{Q}_h / \tilde{c}_p$, and \tilde{Q}_h is

the heat released by combustion of 1 kg of fuel [Jkg^{-1}]. The combustion time scale has been chosen exactly as the acoustic time scale (i.e., $t_{ac} = t_c$). This is a good assumption as long as $M\bar{L}_a/\bar{H} = 1$ (compact flame and low Mach number assumptions). The nondimensional length of the combustion domain along ξ is $L_c = \bar{L}_c/\bar{H}$. The Péclet number is the ratio between the diffusion and convective time scales, $Pe = \bar{U}_0\bar{H}/D$, where D is the (constant) mass diffusion coefficient.

Appendix B: Numerical Discretization With Galerkin Method

The partial differential equations are discretized into a set of ordinary differential equations by picking an orthogonal basis that matches the boundary conditions. The basis functions are the eigenfunctions of the undamped acoustic system when the heat source is absent. This procedure, often used in thermoacoustics, is also known as the Galerkin method. The acoustic variables are expressed as

$$u(x, t) = \sum_{j=1}^N \eta_j(t) \cos(j\pi x), \quad p(x, t) = - \sum_{j=1}^N \left(\frac{\dot{\eta}_j(t)}{j\pi} \right) \sin(j\pi x) \quad (\text{B1})$$

We implicitly make use of a zero Mach number assumption with the above acoustic discretization. Moreover, a compact heat source causes a jump in the base-state temperature and, accordingly, the mean quantities. This changes the acoustic impedance and might have a nonnegligible effect on acoustics (for further elaboration, see Nicoud and Wieczorek [27] and Magri and Juniper [14,15]). These changes in mean quantities are not represented by the Galerkin expansion we used. Our representation, however, is sufficiently accurate for our purposes, because the temperature jump in the Rijke tube is typically small.

As far as the diffusion flame is concerned, the variable z is discretized as follows:

$$z = \sum_{m=1}^M \sum_{n=0}^N \cos(n\pi\eta) \sin \left[\left(m - \frac{1}{2} \right) \frac{\pi\xi}{L_c} \right] G_{mn}(t) \quad (\text{B2})$$

Hence, the discretized thermoacoustic problem can be arranged in the state-space representation.

Appendix C: Steady Solution of the Infinite-Rate Chemistry Diffusion Flame

The analytical solution of Eq. (7) with the relevant boundary conditions obtained via separation of variables is

$$\bar{Z} = \alpha + \frac{2}{\pi} \sum_{n=1}^{+\infty} \frac{\sin(n\pi\alpha)}{n(1+b_n)} \cos(n\pi\eta) [\exp(a_{n1}\xi) + b_n \exp(a_{n2}\xi)] \quad (\text{C1})$$

where

$$a_{n1} \equiv \frac{Pe}{2} - \sqrt{\frac{Pe^2}{4} + n^2\pi^2}, \quad a_{n2} \equiv \frac{Pe}{2} + \sqrt{\frac{Pe^2}{4} + n^2\pi^2} \quad (\text{C2})$$

$$b_n \equiv - \frac{a_{n1}}{a_{n2}} e^{-2 \left(\sqrt{\frac{Pe^2}{4} + n^2\pi^2} \right) L_c} \quad (\text{C3})$$

Note that, if $L_c \gg 1$, then $b_n \sim 0$.

References

- [1] Lieuwen, T. C., and Yang, V., 2005, *Combustion Instabilities in Gas Turbine Engines*, (Progress in Astronautics and Aeronautics, Vol. 210), AIAA, Reston, VA.
- [2] Hill, D. C., 1992, "A Theoretical Approach for Analyzing the Restabilization of Wakes," NASA Technical Memorandum No. 103858.
- [3] Giannetti, F., and Luchini, P., 2007, "Structural Sensitivity of the First Instability of the Cylinder Wake," *J. Fluid Mech.*, **581**, pp. 167–197.
- [4] Marquet, O., Sipp, D., and Jacquin, L., 2008, "Sensitivity Analysis and Passive Control of Cylinder Flow," *J. Fluid Mech.*, **615**, pp. 221–252.
- [5] Sipp, D., Marquet, O., Meliga, P., and Barbagallo, A., 2010, "Dynamics and Control of Global Instabilities in Open-Flows: A Linearized Approach," *ASME Appl. Mech. Rev.*, **63**(3), p. 030801.
- [6] Chandler, G. J., Juniper, M. P., Nichols, J. W., and Schmid, P. J., 2012, "Adjoint Algorithms for the Navier-Stokes Equations in the Low Mach Number Limit," *J. Comput. Phys.*, **231**, pp. 1900–1916.
- [7] Balasubramanian, K., and Sujith, R. I., 2008, "Thermoacoustic Instability in a Rijke Tube: Non-Normality and Nonlinearity," *Phys. Fluids*, **20**, p. 044103.
- [8] Juniper, M. P., 2011, "Triggering in the Horizontal Rijke Tube: Non-Normality, Transient Growth and Bypass Transition," *J. Fluid Mech.*, **667**, pp. 272–308.
- [9] Magri, L., and Juniper, M. P., 2013, "Sensitivity Analysis of a Time-Delayed Thermo-Acoustic System Via an Adjoint-Based Approach," *J. Fluid Mech.*, **719**, pp. 183–202.
- [10] Burke, S. P., and Schumann, T. E. W., 1928, "Diffusion Flames," *Combust. Symp.* **20**(10), pp. 998–1004.
- [11] Tyagi, M., Chakravarthy, S. R., and Sujith, R. I., 2007, "Unsteady Response of a Ducted Non-Premixed Flame and Acoustic Coupling," *Combust. Theory Modell.*, **11**, pp. 205–226.
- [12] Tyagi, M., Jamadar, N., and Chakravarthy, S. R., 2007, "Oscillatory Response of an Idealized Two-Dimensional Diffusion Flame: Analytical and Numerical Study," *Combust. Flame*, **149**, pp. 271–285.
- [13] Balasubramanian, K., and Sujith, R. I., 2008, "Non-Normality and Nonlinearity in Combustion-Acoustic Interaction in Diffusion Flames," *J. Fluid Mech.*, **594**, pp. 29–57.
- [14] Magri, L., and Juniper, M. P., "Adjoint Sensitivity Analysis of Ducted Diffusion Flames for Control of Thermo-Acoustic Instabilities," *J. Fluid Mech.* (submitted).
- [15] Magri, L., and Juniper M. P., 2013, "Using Direct and Adjoint Eigenfunctions to Find Optimal Control Strategies in Thermo-Acoustics," Non-Normal and Nonlinear Effects in Aero- and Thermoacoustics (n31) Conference, München, Germany, June 18–21.
- [16] Magri, L., Balasubramanian, K., Sujith, R. I., and Juniper, M. P., 2013, "Non-Normality in Combustion-Acoustic Interaction in Diffusion Flames: A Critical Revision," *J. Fluid Mech.* (submitted).
- [17] Heckl, M., 1990, "Nonlinear Acoustic Effects in the Rijke Tube," *Acustica*, **72**, pp. 63–71.
- [18] Matveev, I., 2003, "Thermo-Acoustic Instabilities in the Rijke Tube: Experiments and Modeling," Ph.D. thesis, CalTech, Pasadena, CA.
- [19] Stow, S. R., and Dowling, A. P., 2001, "Thermoacoustic Oscillations in an Annular Combustor," ASME Turbo Expo, Paper No. 2001-GT-0037.
- [20] Poinso, T., and Veynante, D., 2001, *Theoretical and Numerical Combustion*, Edwards, Ann Arbor, MI.
- [21] Chu, B. T., 1963, "Analysis of a Self-Sustained Thermally Driven Nonlinear Vibration," *Phys. Fluids*, **6**(11), p. 1638.
- [22] Rayleigh, J. W. S., 1878, "The Explanation of Certain Acoustical Phenomena," *Nature*, **18**, pp. 319–321.
- [23] Shapiro, A. H., 1953, *The Dynamics and Thermodynamics of Compressible Fluid Flow*, Ronald, New York.
- [24] Dowling, A. P., and Ffowcs Williams, J. E., 1983, *Sound and Sources of Sound*, Ellis Horwood, Chichester, UK.
- [25] Culick, F. E. C., 2006, "Unsteady Motions in Combustion Chambers for Propulsion Systems," RTO AGARDograph Paper No. AG-AVT-030.
- [26] Illingworth, S. J., Waugh, I. C., and Juniper, M. P., 2013, "Finding Thermoacoustic Limit Cycles for a Ducted Burke-Schumann Flame," *Proc. Combust. Inst.*, **34**(1), pp. 911–920.
- [27] Nicoud, F., and Wieczorek, K., 2009, "About the Zero Mach Number Assumption in the Calculation of Thermo-Acoustic Instabilities," *Int. J. Spray Combust. Dyn.*, **1**(1), pp. 67–111.